Electronic Supplementary Material (ESI) for Nanoscale.

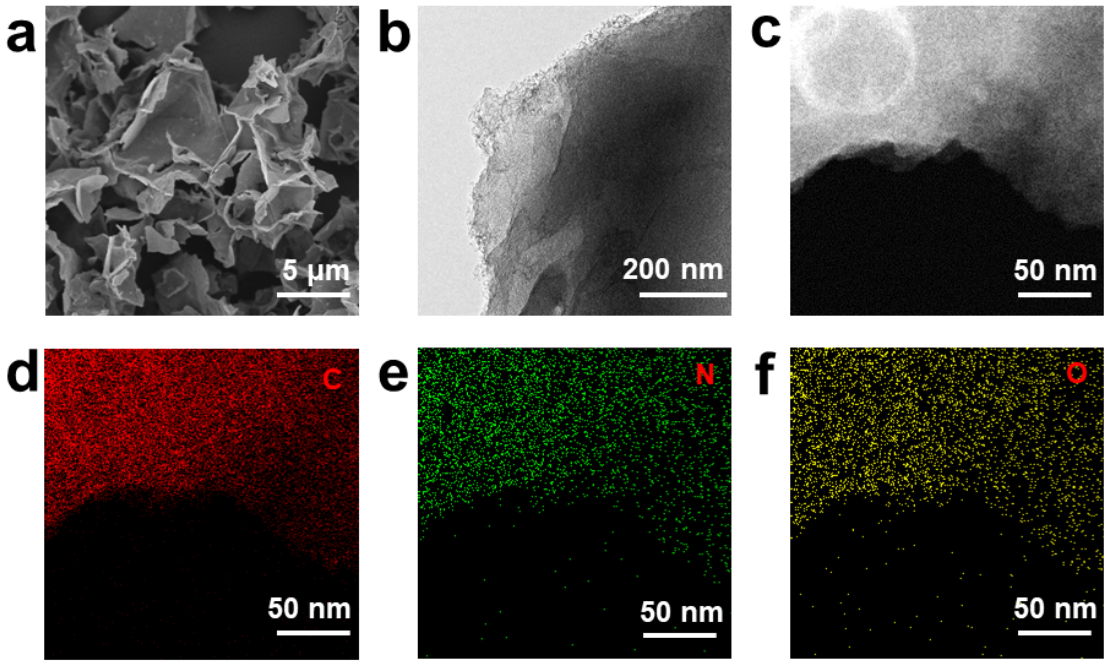

Figure S1. (a) SEM images. (b) HRTEM image. (c)-(f) Elemental mapping of NC catalyst.

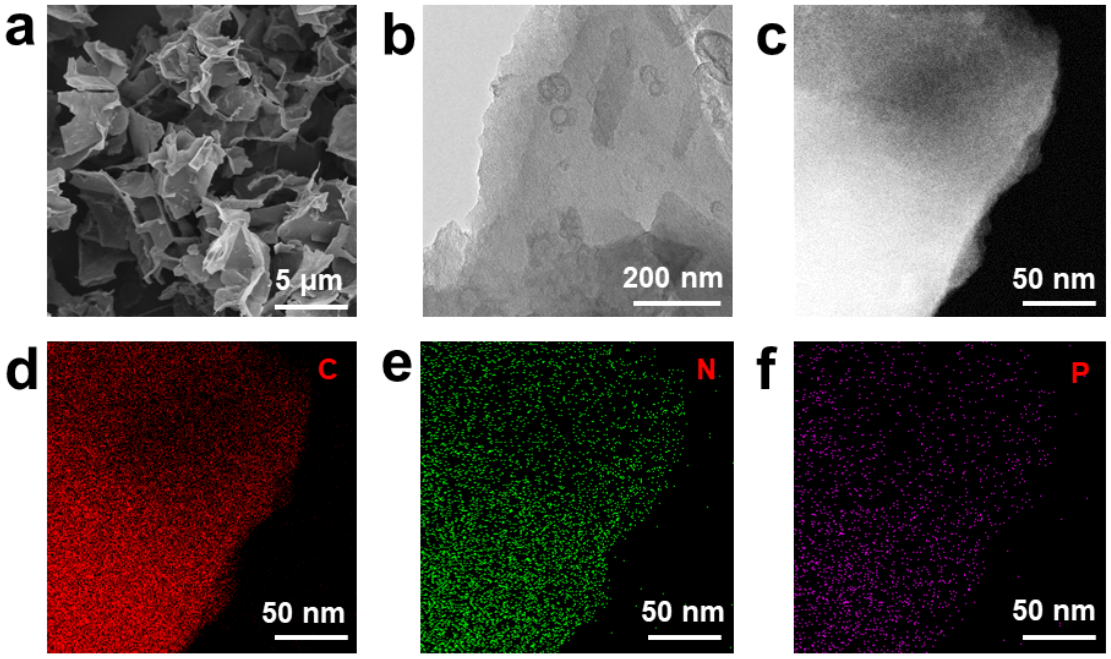

Figure S2. (a) SEM images. (b) HRTEM image. (c)-(f) Elemental mapping of NPC catalyst.

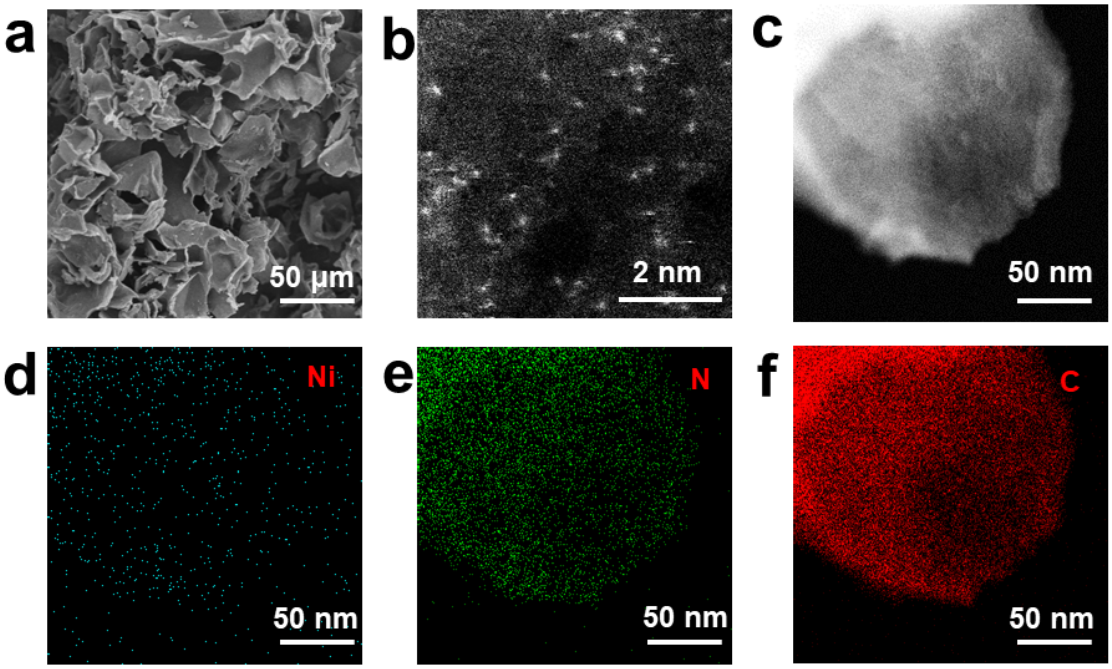

Figure S3. (a) SEM images. (b) HAADF–STEM image. (c)-(f) Elemental mapping of Ni-NC catalyst.

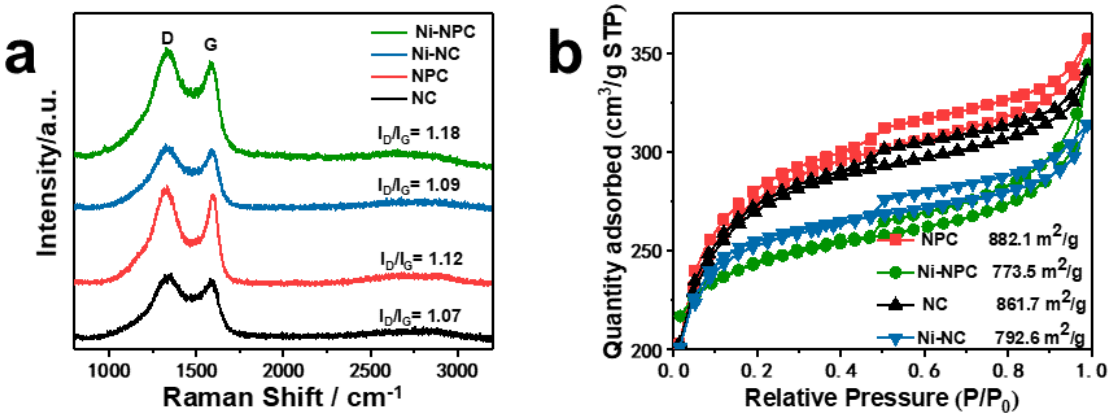

Figure S4. (a) Raman spectra and (b) Nitrogen adsorption-desorption isotherms for the NC, NPC, Ni-NC and Ni-NPC samples.

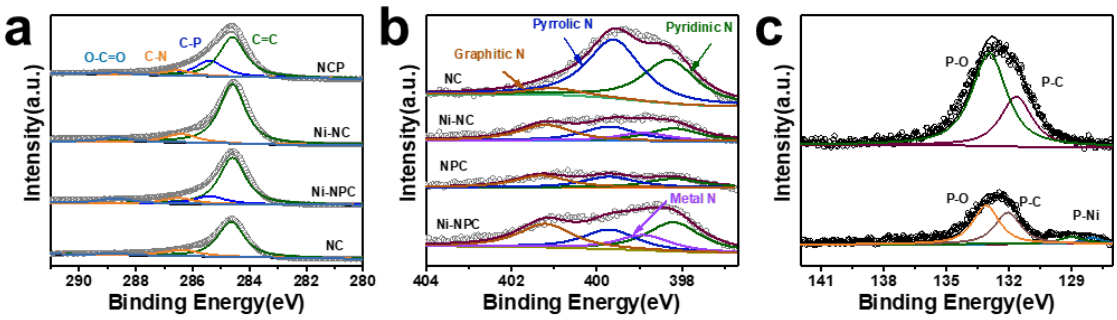

Figure S5. (a) Deconvoluted, high-resolution C 1s XPS spectra, (b) Deconvoluted, high-resolution N 1s XPS spectra and (c) Deconvoluted, high-resolution P 2p XPS spectra of different samples.

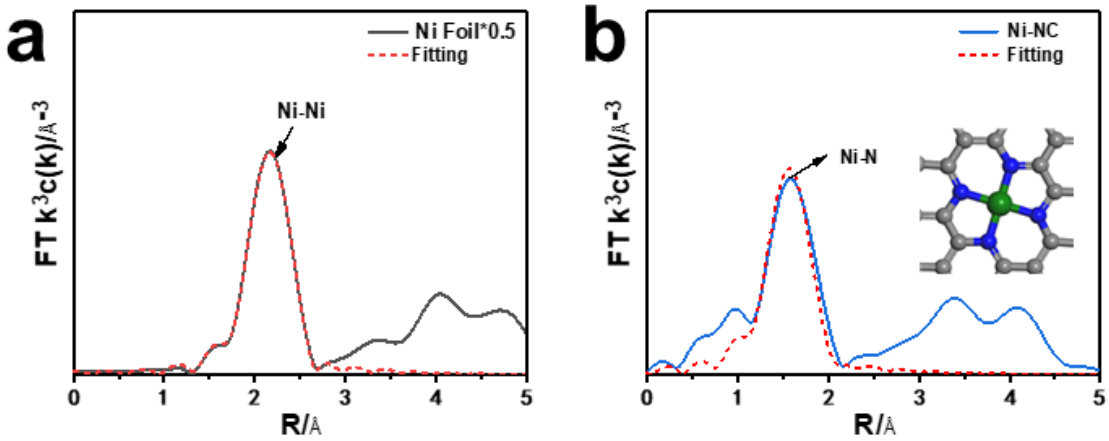

Figure S6. The corresponding EXAFS fitting curves for (a)Ni Foil and (b)Ni-NC samples. The inset shows the proposed structures. (solid lines stand for the as-obtained data and dotted lines denote the fitting curves).

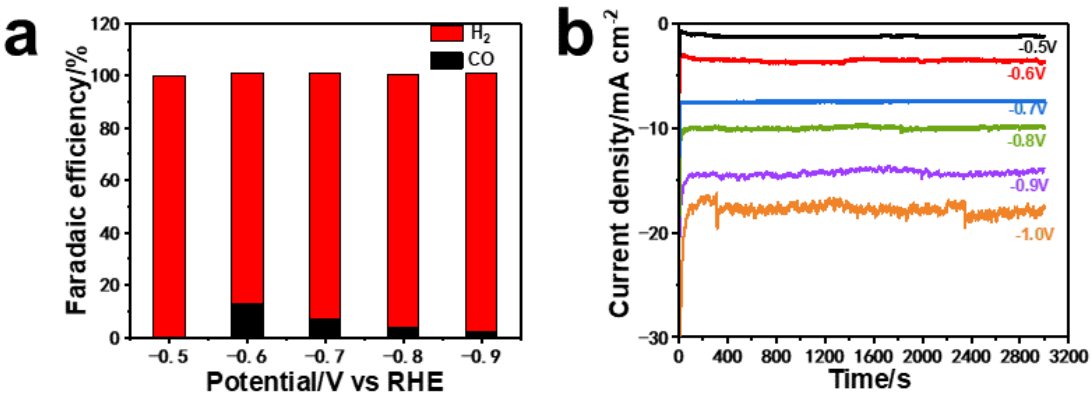

Figure S7. (a) Measured CA curves at different potentials and (b) corresponding Faradaic efficiency for NC catalyst in CO_2-saturated 0.5 M $KHCO_3$.

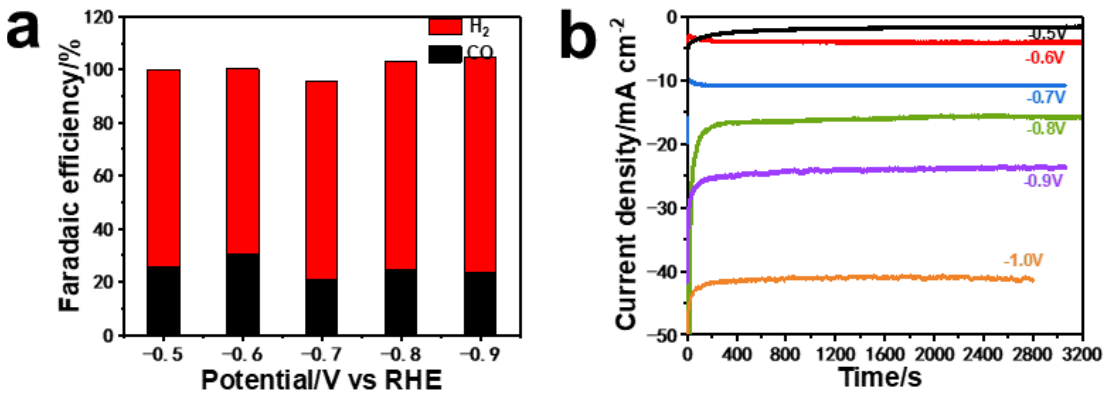

Figure S8. (a) Measured CA curves at different potentials and (b) corresponding Faradaic efficiency for NPC catalyst in CO_2-saturated 0.5 M $KHCO_3$.

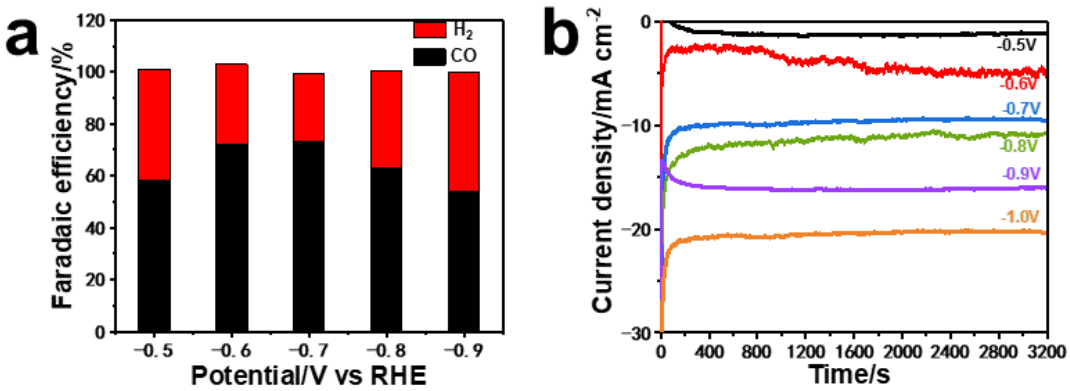

Figure S9. (a) Measured CA curves at different potentials and (b) corresponding Faradaic efficiency for Ni-NC catalyst in CO_2-saturated 0.5 M $KHCO_3$.

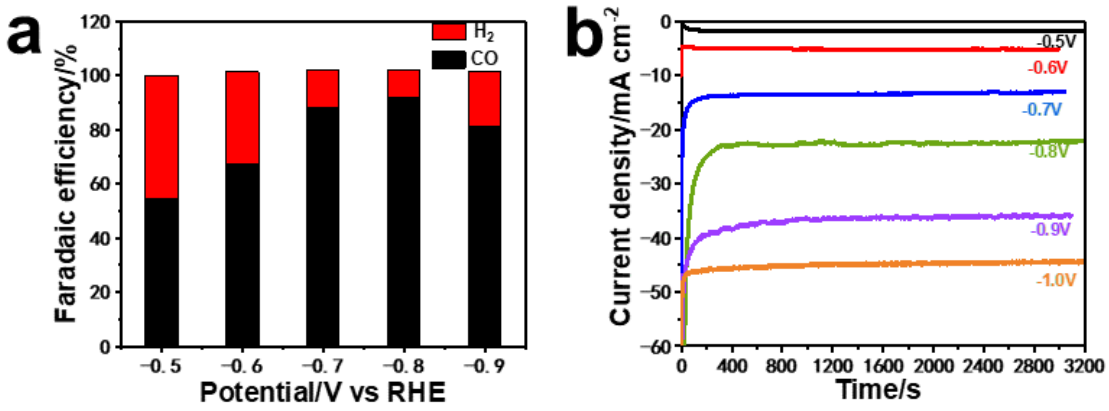

Figure S10. (a) Measured CA curves at different potentials and (b) corresponding Faradaic efficiency for Ni-NPC catalyst in CO_2-saturated 0.5 M $KHCO_3$.

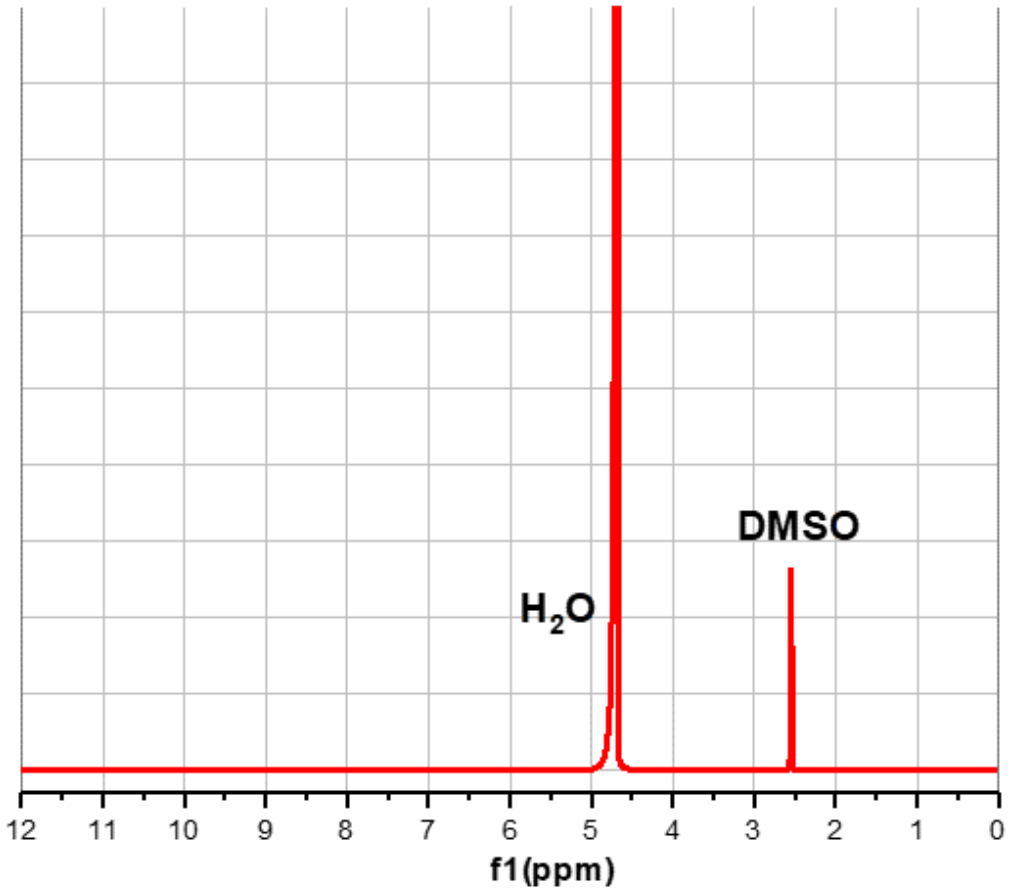

Figure S11. NMR spectrum of the electrolyte for Ni-NPC after 16 h constant potential electrolysis at -0.8 V vs. RHE.

In the NMR spectra, no signal of liquid products (e. g. HCOOH) is observed for Ni-NPC, indicating no liquids are generated at Ni-NPC electrocatalyst under 16 h constant potential electrolysis at -0.8 V vs. RHE.

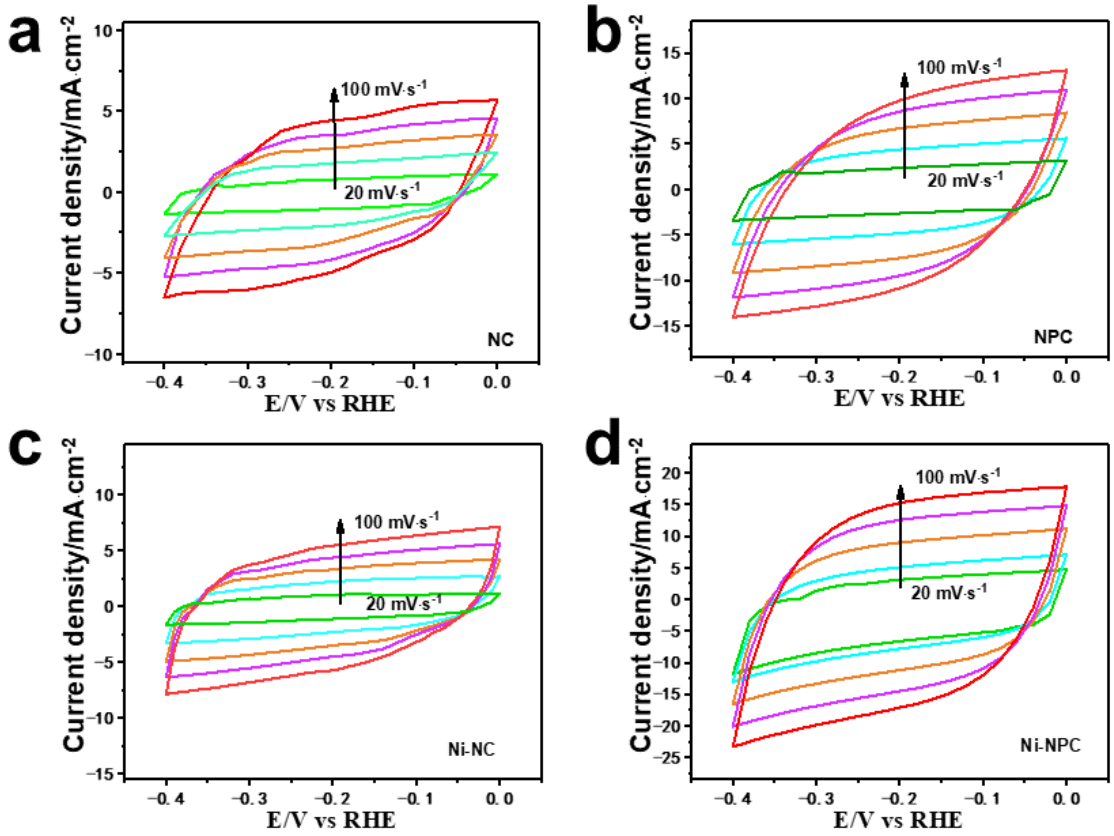

Figure S12. CV curves for a) NC, b) NPC c) Ni-NC and d) Ni-NPC catalysts at different scan rates of 20~100 mV s^{-1} in the potential range of 0.00~0.4 V (vs. RHE).

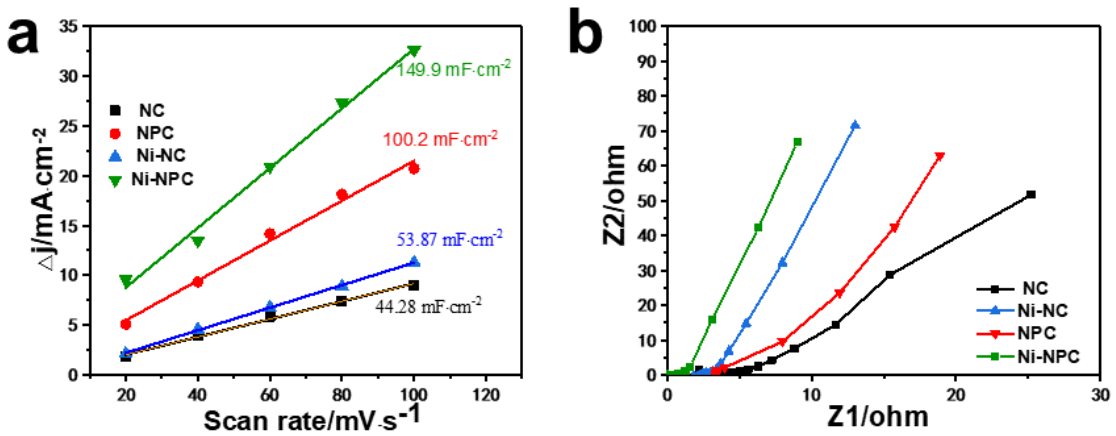

Figure S13. (a) Charging current density differences plotted against the scan rates. (b) Nyquist plots for the samples in CO_2-saturated $KHCO_3$ electrolyte.

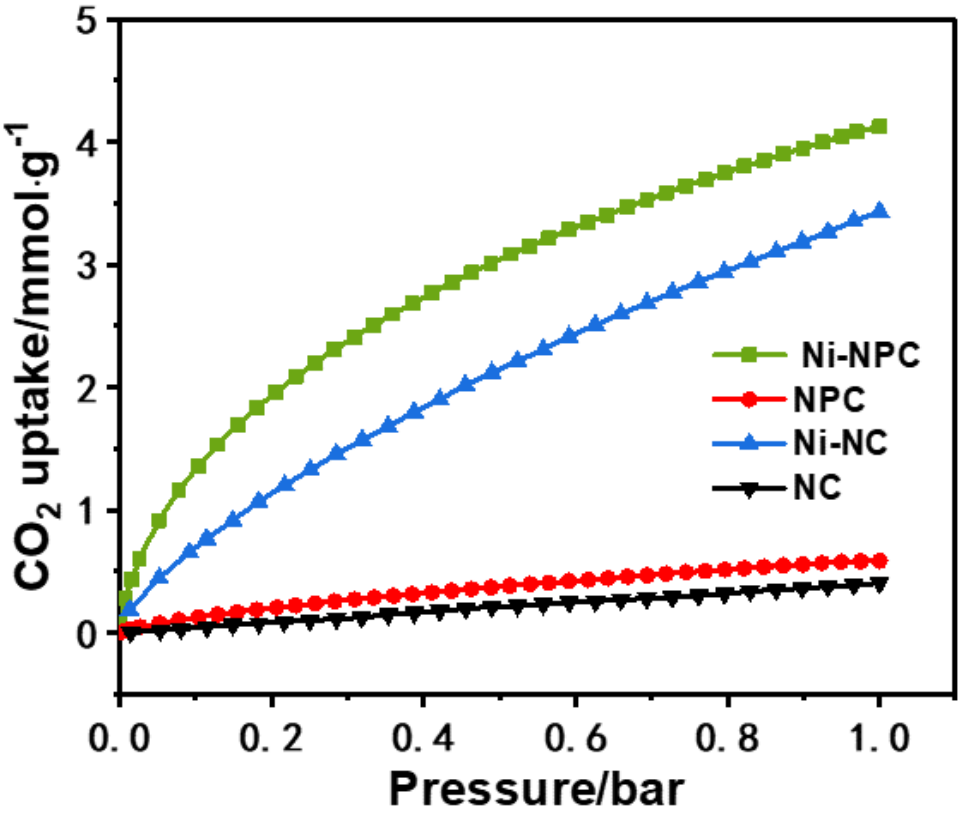

Figure S14. CO_2 adsorption isotherms on different samples.

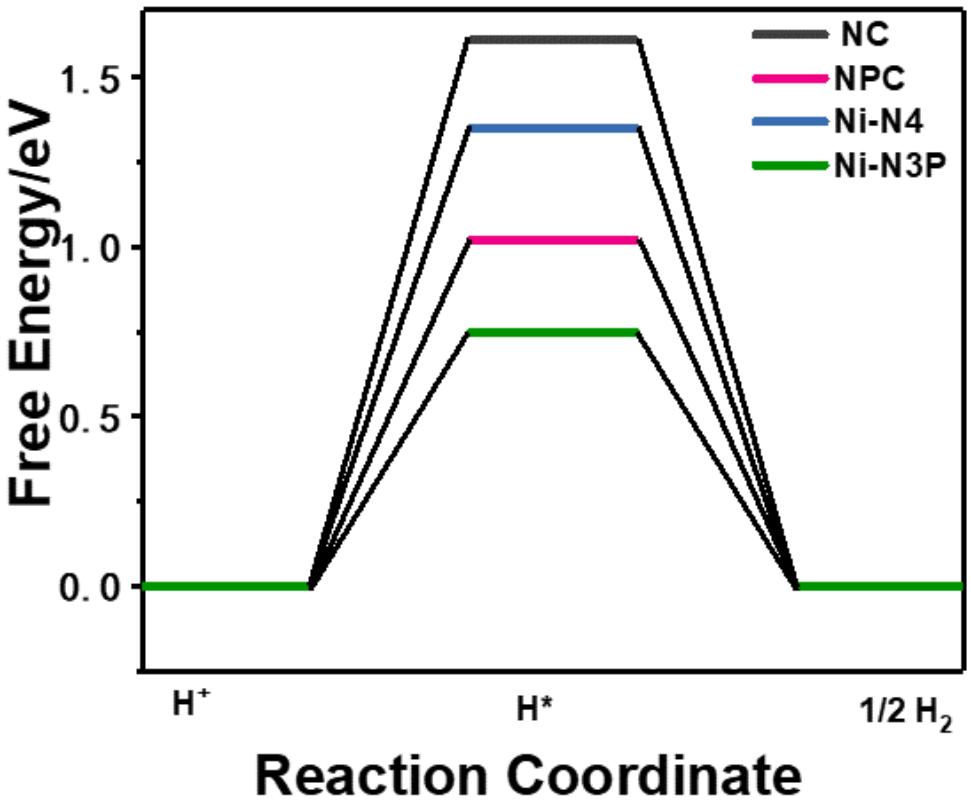

Figure S15. Free energy diagram for HER process in NC, NPC, Ni-N4 and Ni-N3P active sites.

Table S1. XPS analysis on element content of NC, NPC, Ni-NC and Ni-NPC catalysts.

	Element content (at%)				
Sample	C	N	O	Ni	P
Ni-NC	92.23	4.06	3.30	0.42	/
Ni-NPC	81.48	8.24	8.77	0.47	1.05
NC	69.13	10.89	19.90	/	/
NPC	85.58	3.06	9.19	/	2.18

Table S2. EXAFS fitting parameters at Ni K-edge various samples.

Sample	Shell	C.N.	R (Å)	$\sigma^2 \times 10^3$ (Å^2)	ΔE (eV)
Ni foil	Ni-Ni	12*	2.48	2.1	6.6
Ni-NC	Ni-N	4	1.94	3.8	1.9
Ni-NPC	Ni-N	3	1.89	6.3	1.8
	Ni-P	1	2.21	5.6	7.7

Table S3. The Bader Charge of NC, NPC, Ni-N4 and Ni-N3P active sites.

	Ni-NC	Ni-NPC	NC	NPC
Ni	**+0.839**	**+0.587**	/	/
N	**-1.124**	**-1.102**	**-1.109**	**-1.119**
P	/	**+1.357**	/	**+1.154**